ELSEVIER

Journal of Molecular Catalysis A: Chemical 193 (2003) 227–236

JOURNAL OF MOLECULAR CATALYSIS A: CHEMICAL

www.elsevier.com/locate/molcata

Modified iron perovskites as catalysts precursors for the conversion of syngas to low molecular weight alkenes

M.R. Goldwasser [a,*], V.E. Dorantes [a], M.J. Pérez-Zurita [a], P.R. Sojo [a], M.L. Cubeiro [a], E. Pietri [a], F. González-Jiménez [b], Y. Ng Lee [b], D. Moronta [b]

[a] *Escuela de Química, Apartado 47102, Los Chaguaramos, Caracas, Venezuela*
[b] *Escuela de Física, Facultad de Ciencias, Universidad Central de Venezuela, Apartado 47102, Los Chaguaramos, Caracas, Venezuela*

Received 15 May 2002; accepted 7 August 2002

Abstract

Five perovskite oxides with the composition $La_{1-x}K_xMn_yFe_{1-y}O_3$ ($0 \leq x, y \leq 0.2$) were synthesized by the co-precipitation method. Techniques such as chemical and XR fluorescence analysis, powder X-ray diffraction (XRD), BET surface area, IR, EPR and Mössbauer spectroscopy were applied to characterize the structural features of the perovskites. The activity of the solids was strongly dependent on the presence of iron carbides. It was observed that K promotes the reducibility of the solid to α-Fe giving rise to more carbide phases. Mn produces a significant increase in alkenes production. The combined presence of both K and Mn ($La_{0.9}K_{0.1}Fe_{0.9}Mn_{0.1}O_{2.9}$) strongly modified the selectivity of the oxides, giving rise to a stable catalyst with high yield of C_2–C_4 alkenes.

Keywords: Iron perovskites; Syngas conversion; Potassium promotion; Manganese promotion; Low alkenes production; Mössbauer spectroscopy

1. Introduction

The unpredictability of crude oil prices, proved over the last three decades, has brought about in recent years renewed interest in the conversion of syngas, especially for the selective production of petrochemical feedstock such as C_2–C_4 alkenes [1–5]. The key factors to have into account are all related to the catalyst [6]. On one hand, the synthesis of new catalysts is object of intensive research [5] and on the other, highly selective catalysts seem to be the challenge for the present century [7]. Due to the lack of selectivity shown by this reaction, the production of low molecular weight alkenes from syngas calls for new catalytic systems to be developed. Complex mixed metal oxides with the perovskite structure and composition ABO_3 have long attracted the interest of chemists, as they exhibit interesting solid-state properties, making the structure very appropriate as model catalysts. One interesting feature of these complex mixed-oxides is that their catalytic activity can be highly improved by partial substitution on A and/or B sites, with only small changes in the average structure. A and B sites doping, gives rise to $A_1A_2B_1B_2O_3$ type oxides, that improve the catalytic activity [8,9,12–16,18,20]. B cations could be partially reduced to well-disperse metallic species supported on the perovskite, which

* Corresponding author. Fax: +58-212-239-21-62.
E-mail address: mgoldwas@reacciun.ve (M.R. Goldwasser).

1381-1169/02/$ – see front matter
PII: S1381-1169(02)00472-7

make them ideal catalyst precursors for a series of reactions such as syngas conversion.

Fe is an active component in synthesis gas conversion; the use of this element in catalysts for the Fischer–Tropsch synthesis (FTS) has been extensively studied [2–4,21–37]. For iron-based catalysts, activity in syngas conversion appears to correlate better with the extent of Fe reduction, a parameter related to the degree of metal-support interaction, rather than with dispersion, which is related to metal crystallite surface structure [21,24].

It is well known that the addition of promoters to supported metal catalysts has an effect on the light alkenes selectivity [4,21–24]. Bartholomew [21] and Dry [4,22] attributed the increase of the C/H surface ratio produced by K to both a donation of electron density to Fe as well as a local chemical interaction at the metal-promoter interface. Mn has also received a great deal of attention due to the observed increase in the low alkenes ratio, together with a decrease in methane formation, on Mn promoted iron catalysts [25–36]. However, the nature of the effect of Mn on iron has been more controversial, and it is still not clear. The existence of an electronic like interaction [27] and the formation of solid solutions between iron and manganese, have been claimed [28–30]. High selectivity to low molecular weight alkenes has been observed over K and/or Mn iron promoted catalytic systems [31–36]. Oades and Morris [31] patented the use of Fe-Mn supported on silica and magnesia and on Fe-K and Fe over MnO for the production of C_2–C_4 hydrocarbons. Barrault and Renard [32] obtained an active and selective catalyst for low alkenes production from syngas, using a catalyst prepared from iron acetyl acetonate, $Fe(ACAC)_3$ on MnO. The catalytic conversion was 10%. Kreitman and Baerns [33] with Fe/MnO obtained a conversion lower than 10%. Venter and others [34,35] reported well-dispersed, carbon-supported Fe-Mn and KFeMn catalysts, prepared from mixed metal clusters as very active for CO hydrogenation while at the same time retaining a very high selectivity for light alkenes.

While a great number of promoted iron-based catalytic systems has been studied [2–4,21–37,45–50], our system focuses on the use of Fe-based perovskite-like oxides as precursors to in situ produce K-Mn promoted iron catalysts for syngas conversion.

In this work, we try to find trends between solid compositions of a series of La-Fe perovskite-like oxides, used as catalyst precursors, and the activity/selectivity pattern in *syngas conversion*. To achieve this, both La and Fe cations *in the perovskite precursor* were partially substituted by K and/or Mn as promoters in order to control the selectivity of the reaction and to enhance low molecular weight alkenes formation.

2. Experimental

2.1. Catalyst preparation

Five perovskite-like oxides were prepared by doping the matrix $LaFeO_3$ with K and/or Mn, to obtain a series of oxides of general formula: $La_{1-x}K_xFe_{1-y}Mn_yO_3$ (x and y were varied from 0 to 0.2). The solids are named as shown in Table 1.

Catalysts were prepared by the co-precipitation method dissolving the nitrate salts in water using NH_4OH as precipitating agent. The precursor precipitates were dried overnight at 413 K, pressed at 10 ton m^{-2} and calcined at 923 K for 12 h in flowing air (50 ml min^{-1}). For all solids, the effect of pre-treatment

Table 1
Chemical analysis and BET surface areas

Solid	Chemical formula	La (wt.%)	Fe (wt.%)	K (wt.%)	Mn (wt.%)	Surface areas ($m^2\ g^{-1}$)
LaFe	$LaFeO_3$	69.0 (67.1)	23.0 (32.9)	–	–	13
LaKFe 1	$La_{0.9}K_{0.1}FeO_{2.9}$	68.0 (63.4)	29.4 (34.5)	0.5 (2.1)	–	7
LaKFe 2	$La_{0.8}K_{0.2}FeO_{2.8}$	60.0 (59.4)	30.0 (36.4)	2.0 (4.2)	–	3
LaMnFe	$LaMn_{0.2}Fe_{0.8}O_3$	69.0 (67.2)	17.0 (26.3)		2.1 (6.5)	37
LaKMnFe	$La_{0.9}K_{0.1}Mn_{0.1}Fe_{0.9}O_{2.9}$	69.0 (63.5)	19.7 (31.1)	1.8 (2.0)	1.5 (3.4)	6

Values in parentheses shows theoretical values expressed as oxides.

and of temperature on the conversion/selectivity pattern was studied. The usual protocol was as follows: calcined → reduced → carburated → catalytic test.

2.2. Syngas conversion reactions

Before reaction, the perovskite oxides were submitted to treatment with H_2 (30 ml min^{-1} $gcat^{-1}$) at 723 K during 16 h (reduced catalysts), followed by exposure to CO (10 ml min^{-1} $gcat^{-1}$) leaved at 423 K for 8 h and then at 623 K for 14 h (carburated catalysts). Catalytic tests were performed in a continuous flow system with a fixed-bed stainless steel reactor (20 cm, 0.7 cm i.d.) using 1.5 g of catalyst, under 1.1 MPa, 553 K, $H_2/CO = 2$ and 5% N_2 as internal standard. Effluent gases were analyzed periodically by gas chromatography. Permanent gases (N_2, CO, CH_4 and CO_2) were analyzed on line with a Varian 3300 gas chromatograph equipped with a thermal conductivity detector using a CTR-I Alltech packed column. C_1–C_7 hydrocarbons were analyzed in a Perkin-Elmer Sigma 3B chromatograph with a flame ionization detector and a Durapak *n*-octane Porasil packed column. CO conversions were determined using nitrogen as an internal standard, and chromatograms were correlated through methane. Selectivities were obtained based on CO converted.

2.3. Characterization

The sample compositions were determined by inductively coupled plasma emission spectroscopy (ICEPS) using a Perkin-Elmer ICP/5500 instrument to determine Fe, K and Mn, while La was analyzed by X-ray fluorescence analysis (Phillips, PW 1410). The surface areas of the materials were measured on a Micromeritics Flowsorb II 2300 analyzer using nitrogen adsorption at 77 K and the BET method. Prior to the adsorption measurements, the samples were out gassed at 573 K for 3 h. Powder X-ray diffraction (XRD) (Phillips PW 1390, Cu Kα radiation, $\lambda = 1.54178$ Å, flat plate sample, $0^\circ < 2\theta < 70^\circ$) and infrared spectroscopy (Perkin-Elmer 283B, KBr/sample = 5/1) were carried out at room temperature to ascertain formation of the perovskite structure, phase purity and cell parameters. To determine the degree of Fe reduction and formation of different iron phases, catalysts were analyzed after pre-treatment and reaction by EPR (E-line Century Series, X band, 9.5 GHz and 77 K) and by Mössbauer spectroscopy at room temperature using ^{57}Co in a Pd matrix as a source of γ-ray. About 0.2 g of the samples were rapidly placed on an aluminum holder and sealed with epoxy, in order to diminish the probability of reoxidation. Spectra were fitted by means of a least squares program.

3. Results and discussion

3.1. Catalyst characterization

3.1.1. Chemical analysis and surface area measurements

Table 1 lists the synthesized perovskite oxides, their chemical formula and surface areas. In general, the La and Fe chemical composition of the perovskite oxides are within the expected values. However, Mn and specially K content are always lower than the theoretical values. The low K content observed for the K-doped solids could be explained in terms of the volatility of K_2O at high temperature. BET surface areas lie in the range 3–37 m^2 g^{-1} which is not surprising, since preparation of perovskite oxides by solid-state reaction of the precursor oxides, to form the characteristic $A_1A_2B_1B_2O_3$ structure, requires long exposure to high temperatures leading to low surface area solids [8,9,14–16,20]. As expected, the surface areas shown by K containing oxides were lower, due to the sintering character of K [36]. An increase in the surface area of the lanthanum–iron perovskite (LaFe) when Mn is introduced in the perovskite, from 13 to 37 m^2 g^{-1}, was observed. Similar behavior has also been reported by Hansen et al. [10] and Sinquin et al. [17] when working with LaSrFeMn and LaCoMn perovskites respectively. However, in our work a relationship between surface area of the precursor perovskites and activity was not observed, since the perovskite precursor with the higher surface area (LaMnFe) showed the lower activity.

3.1.2. IR spectroscopy and X-ray diffraction

All the perovskite oxides showed the usual IR spectrum [38] with two strong and broad bands centered at 600 and 400 cm^{-1}. The high frequency band, which corresponds to a stretching vibration due to a change in length of a B–O bond [39,40] shifted to higher wave

numbers on doping, corroborating that solid solution has been obtained and that doping has been successful.

The observed XRD spectra were the typical for a perovskite structure with alternating strong and weak peaks (Fig. 1). Some precursors, such as single oxides or not identified by-products, were also observed, especially in the more complex solid solutions. In particular, peaks signaled by asterisks in Fig. 1, has been assigned to a lanthanum oxide species, most probably $La(OH)_3$, as this sub-spectrum can be indexed with the reported most strong lines for that species [41]. Bernal et al. [42] and Squire et al. [43] have also pointed out the presence of $La(OH)_3$ on the surface of lanthanum oxide. As K and Mn replaced La and Fe, the intensity of $La(OH)_3$ peaks increases being higher for LaKMnFe. Because of the hydrophilic character of La_2O_3, water adsorption during sample handling could be responsible for the presence of $La(OH)_3$. The formation of La_2O_3 and $La(OH)_3$ is in agreement with the high lanthanum content observed by chemical analysis (Table 1).

At room temperature, all synthesized solids could be indexed with an orthorhombic $LaFeO_3$ symmetry by JCPDS (file 37-1493) [44], with cell parameters shown in Table 2. The observed cell parameters values for the original LaFe perovskites, are in good agreement with those reported by Geller and Wood [45]. Although no significant changes can be easily observed in the diffraction pattern after doping with K^+ and Fe^{3+}, a systematic shifting of the lines to 2θ higher values was shown, associated to an observed cell dimension decrease. However, this behavior is unexpected since the ionic radii of K^+ and Mn^{3+} are larger than that of La^{3+} and Fe^{3+}, respectively. Lost of oxygen to form oxygen vacancies (for charge compensation on doping) together with a probable change in manganese oxidation state (Mn^{3+}/Mn^{4+}) could account for this phenomenon [46].

Table 2
Cell parameters of as-synthesized perovskite-like oxides

Solid	*a* (Å)	*b* (Å)	*c* (Å)	Cell volume (Å^3)
LaFe	5.50 (7)	7.83 (4)	5.52 (3)	237.7
LaKFe 1	5.49 (4)	7.82 (5)	5.51 (4)	236.6
LaKMnFe	5.47 (7)	7.81 (4)	5.30 (2)	226.8

Values in parentheses refers to the uncertainty in the last digit.

The similarity of the diffractograms and the systematic line shift after doping, together with the reduction in cell dimensions, corroborated the solid solution formation and the presence of perovskite-like oxides.

3.1.3. Mössbauer spectroscopy

As previously mentioned, being the perovskite oxide a very stable structure [9,16,19], it is expected that iron in the perovskite could only be partially reduced to the metallic species. This observation was monitored by Mössbauer spectroscopy comparing the spectra before and after reduction and after carburization and reaction. It can be observed that the as-synthesized perovskites (Fig. 2a and c for LaFe and LaKFe 1, respectively) showed only a symmetric sextuplet characteristic of magnetic iron in an octahedral (cubic) environment [37,47–51] with hyperfine parameter values, Hpf, presented in Table 3 which correspond to Fe in the perovskite structure. For simplicity, it was named as the perovskite phase Fe (P). After reaction, the spectrum of LaFe perovskite looks nearly unchanged (Fig. 2b). However, some weak lines, attributed to formation of a carbide phase, can be seen in the central zone of the spectrum. Only 11% of the iron (Table 3) is in the form of a carbide phase, with the rest remaining as part of the perovskite structure.

The Mössbauer spectrum and hyperfine parameters of the as-synthesized LaKFe 1 are similar to those of LaFe (Fig. 2c), indicating that only small changes of the original perovskite took place after K doping. However, as the K content increases, the stability of the perovskite structure seems to have decreased, as suggested by the presence of α-Fe after reduction. It is believed that A cations act as electron donors to B cations [11], which seems to be reflected in an increase in iron reducibility. The presence of α-Fe, observed for both K containing perovskites, LaKFe 1 and LaKFe 2 (Fig. 2d, Table 3), was greater than that present in LaFe. The presence of α-Fe led to the formation of iron carbides by treatment with CO and syngas (Fig. 2e and f, Table 3).

Mn doping to produce the species LaMnFe brings about some variation in hyperfine parameters (503 kG compare to 519 kg). In particular, a decrease in Hpf values must be attributed to partial substitution of Fe by Mn, indicating that the environment near Fe has changed by Mn incorporation on the perovskite structure increasing the electron density on Fe. However,

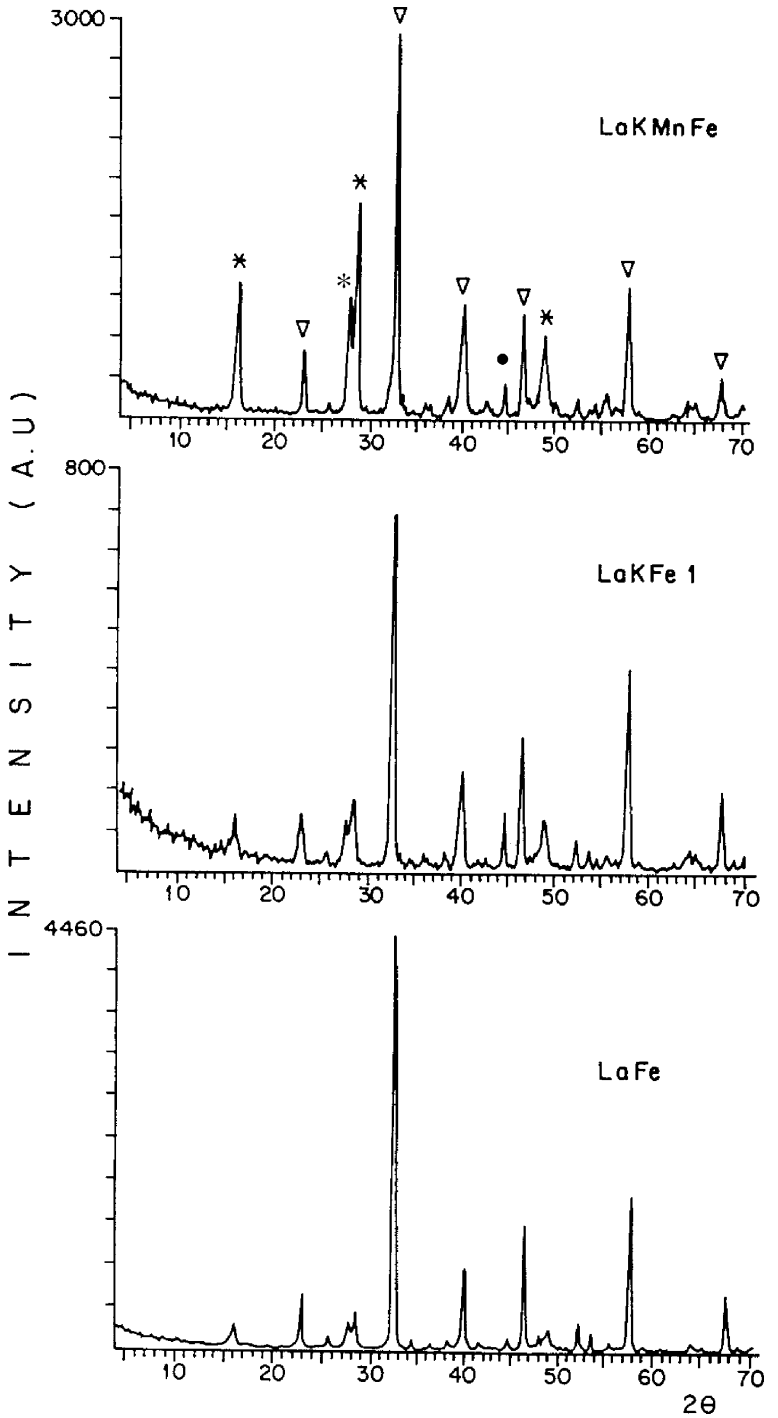

Fig. 1. X-ray diffraction patterns for as-synthesized LaFe, LaKFe 1 and LaKMnFe perovskite-like oxides. (▽) Perovskite-like phases; (∗) $La(OH)_3$; (●) La_2O_3.

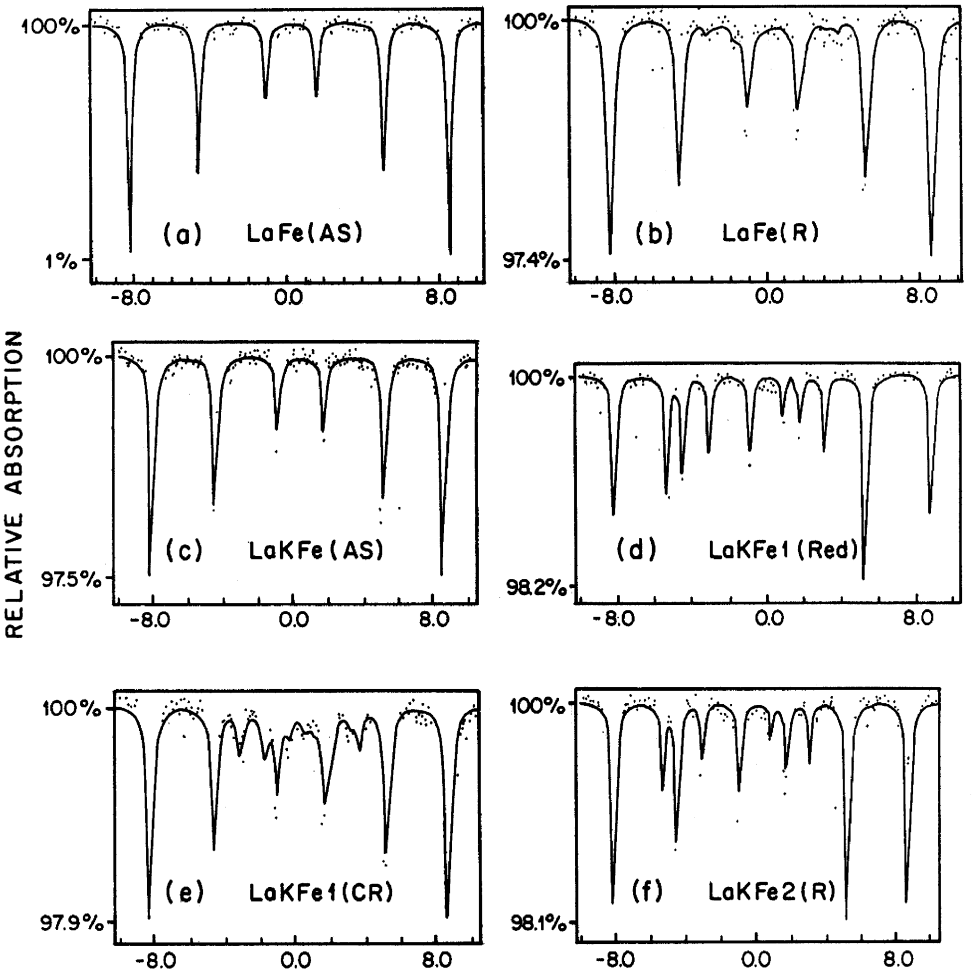

Fig. 2. Mössbauer spectroscopy for LaFe and LaKFe perovskites before and after reduction and reaction. (AS): as-synthesized; (Red): reduced; (R): reacted; (CR): carburated-reacted.

this effect is not reflected in the iron reducibility since only the Fe (P) sextuplet was present in the spectrum. α-Fe or Fe-carbide phases were not observed.

Fig. 3 shows the Mössbauer spectrum for LaKMnFe under different stages of treatment. Three Hpf values for iron are reported for the as-synthesized LaKMnFe (Table 3) because of introducing K and Mn in the original LaFe matrix. Formation of α-Fe can be seen in the spectrum after reduction (36%). The appearance of the Hägg carbide phase increased accordingly (37%). Comparison of Mössbauer results (Table 3) for LaKFe 1 and LaKMnFe perovskites suggests that introduction of Mn produced a further decrease in the stability of LaKFe perovskite. Thus, the proportion of iron in the perovskite phase after reduction and after carburization and reaction was lower for the Mn containing perovskite. The LaKMnFe perovskite seems to be especially susceptible to CO pretreatment or to syngas exposure during reaction. These treatments led to a significant decrease in the proportion of iron in the perovskite phase. Further, incomplete reduction of iron seemed to occur, as indicated by the presence of a Fe_3O_4 phase (Table 3, 30%). Probably, a certain degree of substitution of Mn in the iron oxide lattice increases the difficult of reduction of the iron oxide. It is interesting to point out the coincidence

Table 3
Mössbauer hyperfine parameters

Solid	DI ($mm\,s^{-1}$)	QS ($mm\,s^{-1}$)	Hpf (kG)	Phase	Percentage
LaFe (AS)	0.36	−0.08	519	Fe (P)	100
LaFe (R)	0.36	−0.09	526	Fe (P)	89
	0.25	0.09	213	χ-Fe_5C_2	11
	0.25	0.01	185		
	0.25	0.01	115		
LaKFe 1 (Red)	−0.36	−0.07	522	Fe (P)	74
	−0.01	0.00	329	α-Fe	26
La KFe 1 (CR)	0.36	0.09	529	Fe (P)	74
	0.25	0.09	213	χ-Fe_5C_2	26
	0.25	0.01	185		
	0.25	0.01	115		
La KFe 2 (Red)	0.36	−0.07	525	Fe (P)	59
	−0.01	0.00	330	α-Fe	49
LaKMn (R)	0.34	−0.05	503	Fe (P)	100
LaKMnFe (Red)	0.38	−0.10	511	Fe (P)	39
	0.32	−0.13	483	Fe (P)	25
	−0.01	0.00	324	α-Fe	36
LaKMnFe (CR)	0.25	0.10	213	χ-Fe_5C_2	37
	0.25	0.01	185		
	0.25	0.01	116		
	0.38	0.10	520	Fe (P)	34
	0.32	0.13	490	Fe_3O_4	23
	0.40	0.20	460	Fe_3O_4	6

(P): perovskite; (AS): as-synthesized; (Red): reduced; (R): reacted; (CR): carburated-reacted.

between the amounts of Hägg carbide present in the carburated-reacted (CR) samples to that of α-Fe in the reduced (Red) samples, which are nearly identical (26% for LaKFe 1 and 36–37% for LaKMnFe, Table 3).

3.1.4. EPR spectroscopy

An EPR study was conducted on LaKFe 1 and LaKMnFe perovskite oxides. The as-synthesized and reduced samples did not show any relevant magnetic properties, only a broad signal was observed at ≅10.000 G, typical of the presence of iron phases in different magnetic environments. Similar spectra were observed for the reduced solids. However, when those samples were subjected to treatment under CO or after syngas reaction, a hysteresis loop was observed (Fig. 4). This hysteresis phenomenon is characteristic of the presence of ferromagnetic species in the solid, and since it was observed only in the samples subjected to carburization, this could be related to the presence of Hägg carbides observed by Mössbauer spectroscopy.

3.1.5. Catalytic measurements

Catalytic results are shown in Table 4. The unpromoted LaFe perovskite exhibits poor catalytic properties, even when tested at higher temperature (573 K), with CO conversions around 6%. The higher than 50% CO_2 selectivity value, which is the maximum to be expected from stoichiometric considerations, indicates that this catalyst continues to be reduced under reaction conditions.

K doping of LaFe to produce LaKFe 1 perovskite was seen by Mössbauer spectroscopy to increase Hägg carbide formation. This substantially increases CO conversion (38%) with also a slight increase in the alkenes/alkanes ratio and simultaneously reduces CH_4 and CO_2 production.

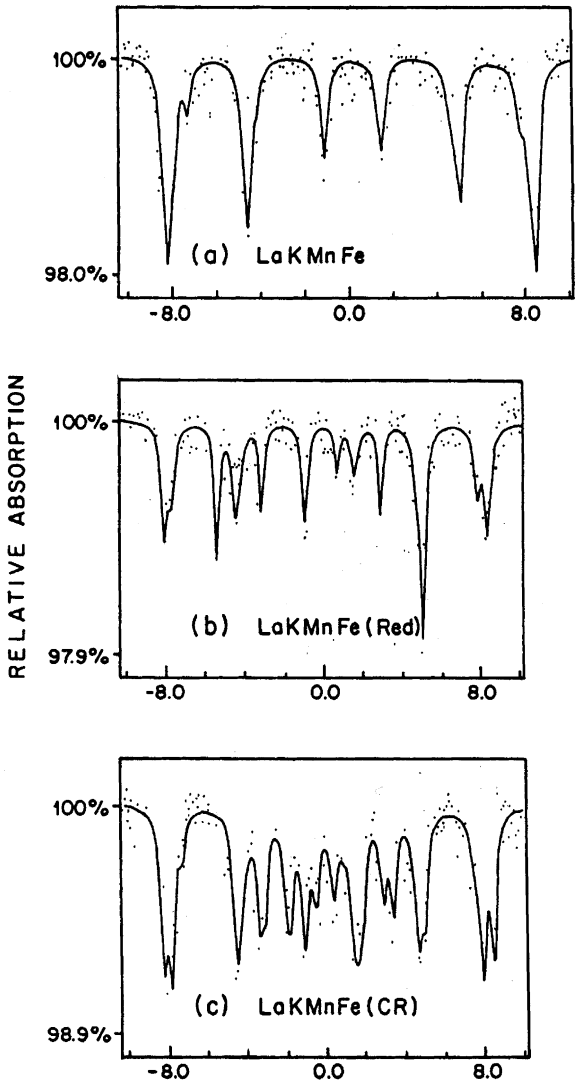

Fig. 3. Mössbauer spectroscopy for LaKMnFe under different treatments. (Red): reduced; (CR): carburated-reacted.

Further doping with K (LaKFe 2) continued to increase the activity of the catalysts (45% CO conversion) with a small reduction in the CO_2 selectivity. The hydrocarbon distribution indicates that the chain growth probability was increased giving rise to more C5+ hydrocarbons at expense of CH_4 and C_2–C_4 hydrocarbons, which could be related to the increase in the Hägg carbides proportion. The slight decrease in the alkenes/alkanes ratio could be attributed to the secondary hydrogenation of alkenes.

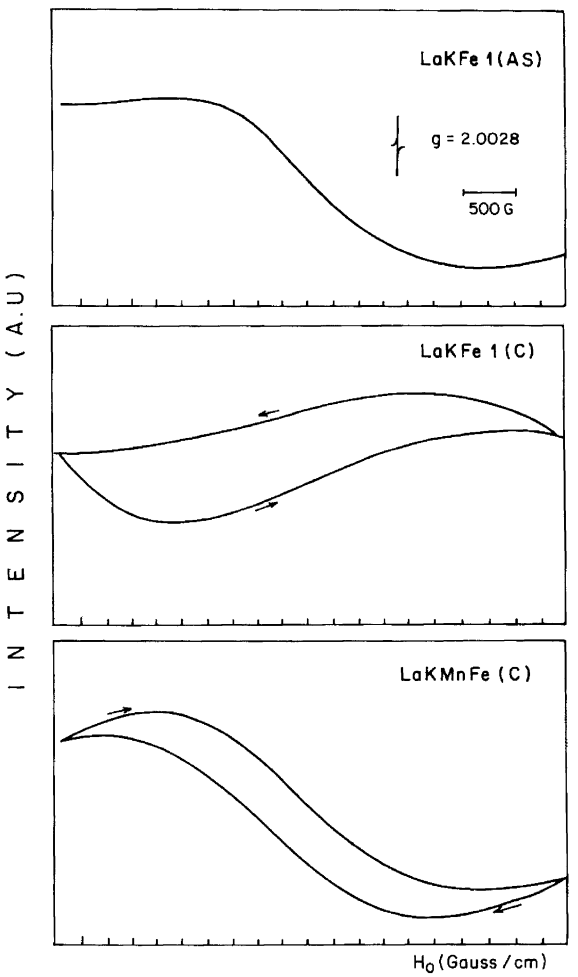

Fig. 4. EPR of LaKFe 1 and LaKMnFe perovskite-like oxides. (AS): as-synthesized; (C): carburated.

The presence of Mn in the LaFe matrix (LaMnFe) did not have a strong effect on the catalytic activity. This behavior is in agreement with the Mössbauer results, since on this solid neither α-Fe nor Fe-carbide phases were observed. A slight increase on the chain growth probability seems to have occurred, together with a decrease in CO_2 selectivity.

The combined presence of K and Mn on the LaFe matrix (LaKMnFe) strongly modified the catalytic behavior of the solid. It produced a stable catalyst that showed a high formation of $C_2^=$–$C_4^=$ alkenes (alkenes/alkanes ratio of 11.4) with a quite low CH_4 production (<10%) as compared to LaFe and the other perovskites.

Table 4
Activity/selectivity of perovskite-like solids

	LaFe (573 K)	LaKFe 1	LaKFe 2	LaMnFe	LaKMnFe
XCO (%)	6	38	45	8	14
SCO_2 (%) (carbon-based)	56.6	38.2	33.4	32.5	30.4
Products (wt.)					
C_1	27.1	21.4	17.7	22.2	9.8
C_2–C_4	66.6	59.1	56.7	60.8	76
C_{5+}	6.3	19.5	25.6	17.0	14.2
$(Alkenes/alkanes)_{C_2–C_4}$	2.7	3.4	2.4	2.4	11.4

$T = 553\,K$; $P = 1.1\,MPa$; tr = 24 h on stream; $W/F = 1.4\,g\,h\,l^{-1}$; $H_2/CO = 2$.

The results indicate that the activity of the perovskite-based catalysts seems to be directly related to the formation of Hägg carbides. In addition, the LaKMnFe perovskite is the precursor of a catalyst with a high selectivity to C_2–C_4 alkenes, in which the promotion of Fe with manganese has to be invoked. The observed relationship between catalytic activity and the abundance of Hägg carbides is in agreement with our previous results for CO and CO_2 hydrogenation on a laterite and a Fe/Al_2O_3 catalysts both unpromoted and promoted with K and Mn [30–50]. In that work, it was established that only those iron species that can be reduced–carburated were able to perform the CO_x hydrogenation. Similarly, Jung and Thomson [51] working with unsupported reduced iron catalysts attributed the observed increase in catalytic activity to the presence of Hägg carbide phases. Dictor and Bell [52] concluded that Hägg carbide or freshly reduced iron, and not magnetite is the active phase for FTS for reduced and unreduced iron oxide.

Compared to other catalytic systems [31–36] the combined perovskite-like oxide $La_{0.9}K_{0.1}Mn_{0.1}Fe_{0.9}O_{2.9}$ looks promising. Further research on this system will be carried on in the near future.

4. Conclusions

The spectral information showed that perovskite-like oxides have been obtained. Similarity of the spectra and systematic shifting in XRD and IR bands demonstrated that K^+ and Mn^{3+} have been incorporated to the matrix of the perovskite structure. Although Mössbauer spectroscopy did not confirm perovskite-like oxide formation by itself, it is clear that a magnetic species, different from α-Fe, hematite or magnetite, has been formed.

Mössbauer and EPR results strongly suggest the presence of a carbide phase. The species present on the more interesting catalysts (LaKFe 1, LaKFe 2 and La KMnFe) were: α-Fe, Hägg carbide, mixed oxides of the perovskite type, and for the LaKMnFe perovskite, a Fe_3O_4 phase was also detected, which seems to be stabilized by the presence of Mn. Although it is difficult to correlate the catalytic properties with the presence of any of them, the presence of Hägg carbides seems to play a primary role. The combined presence of K and Mn in the perovskite-like oxides strongly increases selectivity towards low molecular weight alkenes. The LaKMnFe perovskite is the precursor of an iron catalyst with a high selectivity to C_2–C_4 alkenes.

References

[1] R. Snel, Catal. Rev. Sci. Eng. 29 (1987) 361.
[2] M.R. Goldwasser, M.L. Cubeiro, M.J. Pérez Zurita, C. Franco, Stud. Surf. Sci. Catal. 75 (1993) 2095.
[3] M.R. Goldwasser, F. Navas, M.J. Pérez Zurita, M.L. Cubeiro, E. Lujano, C. Franco, F. González-Jiménez, E. Jaimes, D. Moronta, Appl. Catal. 100 (1993) 85.
[4] M.E. Dry, Catal. Today 71 (2002) 227.
[5] J.R. Rostrup-Nielsen, Catal. Today 71 (2002) 243.
[6] H.H. Kung, E.I. Ko, Chem. Eng. J. 64 (1996) 203.
[7] G.A. Somorjai, K. McCrea, Appl. Catal. A: Gen. 222 (2001) 3.
[8] F.G. Galasso, Structure, Properties and Preparation of Perovskite-Type Compounds, Pergamon Press, Oxford, 1969.
[9] L.G. Tejuca, J.L.G. Fierro, Properties and Applications of Perovskite-Type Oxides, Marcel Dekker, New York, 1992.
[10] K.K. Hansen, E.M. Skou, H. Christensen, T. Turek, J. Catal. 199 (2001) 132.

[11] H.R. Aghabozorg, B.H. Sakakini, A.J. Roberts, J.C. Vickerman, W.R. Flavell, Catal. Lett. 39 (1996) 97.
[12] N. Guilhaume, M. Primet, J. Catal. 165 (1997) 197.
[13] S. Irusta, M.P. Pina, M. Menéndez, J. Santamaría, J. Catal. 179 (1998) 400.
[14] Y. Wu, O. Kawaguchi, T. Matsuda, Bull. Chem. Soc. Jpn. 71 (1998) 563.
[15] M. Stojanovic, R.G. Haverkamp, C.A. Mims, H. Modula, A.J. Jacobson, J. Catal. 165 (1997) 315.
[16] F.G. Galasso, Perovskites and High T_C Superconductors, Gordon and Breach, Amsterdam, 1990.
[17] G. Sinquin, C. Petit, J.P. Hindermann, K. Kiennemann, Catal. Today 70 (2001) 183.
[18] J.B. Goodenough, S.L. Cooper, T. Egami, J.-S. Zhou (Eds.), Localized to Itinerant Electronic Transition in Perovskite Oxides (Structure and Bonding, 98), Springer, Berlin, 2001.
[19] R.J.H. Voorhoeve, in: J.J. Burton, R.L. Garten (Eds.), Advanced Materials in Catalysis, Academic Press, New York, 1977, p. 129.
[20] S. Ponce, M.A. Peña, J.L.G. Fierro, Appl. Catal. B: Environ. 24 (2000) 193.
[21] C.H. Bartholomew, in: L. Guczi (Ed.), New Trends in CO Activation, Elsevier, Amsterdam, Stud. Surf. Sci. Catal. 64 (1991).
[22] M.E. Dry, Appl. Catal. A: Gen. 138 (1990) 319.
[23] R.A. Fiato, E. Iglesia, G.W. Rice, S.L. Soled, Stud. Surf. Sci. Catal. 114 (1998) 339.
[24] F. Zaera, Appl. Catal. A: Gen. 229 (2002) 75.
[25] J.A. Brown Bourzutschky, N. Homs, A.T. Bell, J. Catal. 124 (1990) 52.
[26] G. v d Lee, V. Ponec, Catal. Rev.-Sci. Eng. 29 (1987) 183.
[27] H. Kölbel, K.D. Tillmetz, Deutsches Offent, 2.507.647 (1976).
[28] K.B. Jensen, F.E. Massoth, J. Catal. 92 (1985) 109.
[29] G.C. Maiti, R. Malessa, U. Lochner, H. Papp, M. Baerns, Appl. Catal. 16 (1985) 215.
[30] M.L. Cubeiro, H. Morales, M.R. Goldwasser, M.J. Pérez Zurita, F. González-Jiménez, C. Urbina, Appl. Catal. A: Gen. 189 (1999) 887.
[31] R.D. Oades, S.R. Morris, Patent No. 0166-9834186 (1986).
[32] J. Barrault, C. Renard, Appl. Catal. 14 (1985) 133.
[33] K.M. Kreitman, M. Baerns, J. Catal. 105 (1987) 319.
[34] J.D. Venter, A.A. Chen, J. Phillips, M.A. Vannice, J. Catal. 119 (1989) 451.
[35] J.D. Venter, M.A. Vannice, Catal. Lett. 7 (1990) 219.
[36] T.E. Hoost, J.E. Goodwin Jr., J. Catal. 130 (1991) 283.
[37] L. Guczi, Catal. Rev.-Sci. Eng. 23 (1981) 329.
[38] J.T. Last, Phys. Rev. 105 (1957) 1740.
[39] M. Eibschutz, G. Gorodetsky, S. Shtrikman, D. Treves, J. Appl. Phys. 35 (1954) 3.
[40] C.P. Khattak, D.E. Cox, Mater. Res. Bull. 12 (1977) 463.
[41] JCPDS, International Centre for Diffraction Data, File No. 36-1481 (1994).
[42] S. Bernal, J.A. Díaz, R. García, J.M. Rodríguez-Izquierdo, J. Mater. Sci. 20 (1985) 537.
[43] G.D. Squire, H. Luc, D.C. Puxley, Appl. Catal. 108 (1994) 261.
[44] JCPDS, International Centre for Diffraction Data, File No. 37-1493 (1997).
[45] S. Geller, E.A. Wood, Acta Cryst. 9 (1956) 565.
[46] R. Burch, P.J.F. Harris, C. Pipe, Appl. Catal. A: Gen. 210 (2001) 63.
[47] G. Le Caër, J.M. Dubois, M. Pijolat, V. Perrichon, P. Bussière, J. Phys. Chem. 86 (1982) 4799.
[48] M.L. Cubeiro, M.R. Goldwasser, M.J. Pérez Zurita, F. González-Jiménez, Hyperf. Interact. 93 (1994) 1831.
[49] R.R. Gatte, J. Phillips, J. Catal. 104 (1987) 365.
[50] M.L. Cubeiro, F. González-Jiménez, M.R. Goldwasser, M.J. Pérez-Zurita, E. Pietri, Hyperf. Interact. 134 (2001) 13.
[51] H. Jung, W. Thomson, J. Catal. 139 (1993) 375.
[52] R.A. Dictor, A.T. Bell, J. Catal. 97 (1986) 121.